AIAA JOURNAL
Vol. 43, No. 5, May 2005

# Effects of Inflow Conditions and Forcing on Subsonic Jet Flows and Noise

Christophe Bogey* and Christophe Bailly†
*Ecole Centrale de Lyon, 69134 Ecully, France*

**Large-eddy simulations of a circular jet with a Mach number $M = 0.9$ and a Reynolds number $Re_D = 4 \times 10^5$ are performed to investigate the effects of the inflow conditions on flow development and the sound field. Three parameters are varied in the jet inflow: the forcing amplitude, the shear-layer thickness, and the use of the first modes in the ring vortex excitation involving several azimuthal modes. The most significant modifications in the jet features are found in the latter case: When the first four azimuthal modes are removed from the forcing, the jet develops much more slowly with reduced turbulence intensities, and the jet is quieter. Moreover, links between the sound levels and the turbulence intensity peaks are observed. The downstream sound levels vary like the peak amplitudes of the centerline turbulence intensity, and the sideline sound levels vary like those of the fluctuating radial velocity in the shear layer.**

## Nomenclature

| | | |
|---|---|---|
| $c$ | = | sound velocity |
| $D$ | = | jet diameter |
| $d$ | = | distance between sound source and observation point |
| $f$ | = | frequency |
| $M$ | = | Mach number |
| $Re_D$ | = | Reynolds number |
| $R_{pp}$ | = | azimuthal correlation function of fluctuating pressure |
| $R_{uu}$ | = | azimuthal correlation function of fluctuating velocity |
| $r_0$ | = | jet radius |
| $Sr$ | = | Strouhal number |
| $T$ | = | simulation time |
| $u, v$ | = | axial and radial velocities |
| $u_c$ | = | centerline mean axial velocity |
| $u_j$ | = | inflow jet velocity |
| $x, r, \phi$ | = | cylindrical coordinates |
| $x, y, z$ | = | Cartesian coordinates |
| $x_c$ | = | potential core length |
| $x_0$ | = | axial location of forcing |
| $\alpha$ | = | forcing amplitude |
| $\Delta y$ | = | transverse grid spacing in shear layer |
| $\delta_\theta$ | = | shear-layer momentum thickness |
| $\delta_\omega$ | = | shear-layer vorticity thickness |
| $\theta$ | = | angle from jet axis |
| $\nu$ | = | kinematic molecular viscosity |
| $\lvert\omega\rvert$ | = | vorticity norm |
| $\langle\,\rangle$ | = | time averaging |

*Subscripts*

| | | |
|---|---|---|
| $a$ | = | ambiant |
| $p$ | = | peak value |
| rms | = | root mean square |

*Superscripts*

| | | |
|---|---|---|
| ring | = | unit vortex ring |
| $'$ | = | fluctuating value |

Presented as Paper 2003-3170 at the AIAA/CEAS 9th Aeroacoustics Conference, Hilton Head, SC, 12–14 May 2003; received 7 January 2004; revision received 12 October 2004; accepted for publication 15 October 2004. 

*CNRS Research Scientist, Laboratoire de Mécanique des Fluides et d'Acoustique, UMR Centre National de la Recherche Scientifique 5509, Centre Acoustique, 36, Avenue Guy de Collongue; christophe.bogey@ec-lyon.fr.

†Professor, Laboratoire de Mécanique des Fluides et d'Acoustique, UMR Centre National de la Recherche Scientifique 5509, Centre Acoustique, 36, Avenue Guy de Collongue; christophe.bailly@ec-lyon.fr. Member AIAA.

## I. Introduction

At the end of the 1970s, experiments were conducted to reduce jet noise through artificial shear-layer excitation. Crighton[1] observed contradictory results, including that the broadband noise was suppressed below a Reynolds number $Re_D$ of about $10^5$, but amplified for higher Reynolds numbers $Re_D$. The presence of such a barrier Reynolds number was clarified by noting that its value corresponds to a limit below which the jet exit shear layer is fully laminar.[2] This demonstrates that jet noise mechanisms depend on the shear-layer initial state. These works dealing with excited jets illustrate that jet noise may change according to the initial conditions. This issue must still be investigated to better understand the physics of sound generation. It must also be taken into account for the modeling of inflow conditions in jet noise simulations.

Experimentally, the influence of initial conditions on jet flow has mostly been studied for jets with Reynolds numbers about $10^5 < Re_D < 5 \times 10^5$. In this range, the exit shear layer is expected to be transitional, but the use of tripping devices in the nozzle can make it go fully turbulent. Hill et al.[3] showed that flow characteristics of plane jets were sensitive to changes in the apparatus in the initially laminar case, but not in the turbulent case. A similar sensitivity was found for round jets by Gutmark and Ho,[4] who reported that initial conditions of laminar shear layers were changed by extremely low-level spatially coherent disturbances in the facility. Measures of axisymmetric free shear layers were documented by Hussain and Zedan,[5] Husain and Hussain,[6] and Hussain and Husain[7] for different initial conditions. The parameters in the self-preserving region were shown to be essentially dependent on whether the initial shear layer is transitional or turbulent, whereas the distance required for reaching this region depends noticeably on the initial shear-layer thickness. As for the effects of the initial shear-layer state on the flow itself, they were investigated for round jets by Raman et al.[8] and Xu and Antonia.[9] The jet development was found to be much more rapid in the initially transitional case than in the turbulent case.

The influence of jet exit conditions on subsonic jet noise has also been studied. Bridges and Hussain[10] reported that a circuler jet at $Re_D = 1.5 \times 10^5$ was 2.5 dB quieter when its initial shear layer was tripped. Devices acting on the noise-producing region have been tested with the aim of sound reduction. Simonich et al.[11] used tabs for a circular jet at $Re_D = 1.7 \times 10^6$ to enhance near-field jet mixing, whereas Arakeri et al.[12] used microjets at $Re_D = 5 \times 10^5$ and observed significant lowering in the near-field turbulent intensities. In the two cases, the sound levels decreased by about 2 dB.

In simulations, real exit conditions[2] cannot be reproduced because the discretization of the shear layers leads to a prohibitive number of grid points. Initial conditions must, therefore, be modeled. For jets, the classical approach consists of introducing random perturbations near the inflow to seed the turbulence. These can be issued from a synthetic turbulent field,[13] or be based on the jet azimuthal modes.[14] Their amplitudes are usually set to low values, particularly in noise simulations where spurious waves must be minimized. Great care must be taken to ensure that the artificial inflow conditions do not bias the results, as pointed out by Bodony and Lele[15] regarding forcing using only the first three azimuthal modes of a circular jet. Moreover, whereas Chyczewski et al.[16] observed that the forcing amplitude did not significantly alter the development of a rectangular supersonic jet, Stanley and Sarkar[13] clearly presented the influence of the inflow turbulence intensity and of the shear-layer thickness for a plane subsonic jet. The dependence of the similarity parameters on the initial velocity profile was also shown by Boersma et al.[17] for a circular jet.

In the present paper, the effects of artificial inflow conditions on the plume development and the radiated sound field of a Mach number $M = 0.9$ circular jet are investigated. A Reynolds number of $Re_D = 4 \times 10^5$ is chosen to be above the barrier Reynolds number of $10^5$, in the range of transitional jets where the exit shear layers are not fully turbulent. Such a jet was recently simulated[18,19] using a vortex ring inflow forcing[14] involving the first 16 azimuthal modes. The flow and the sound field obtained directly by large-eddy simulation (LES) were described in detail and compared to relevant measurements. Both correspond to what is expected at a high Reynolds number, supporting the idea that the LES preserves the Reynolds number given by the initial jet conditions. (See, for instance, the study[20] reporting the effects of the subgrid modelings.) In the present work, LES with inflow parameters modified with respect to the earlier simulation[18,19] are performed. The investigated parameters are the forcing amplitude, the initial shear-layer thickness, and the use of the first four azimuthal modes when synthesizing the forcing disturbances. Effects on the jet flow and the noise are shown, and an attempt to discuss noise sources is conducted from the LES data.

In Sec. II, the main features of the numerical procedure and the specifications of the different inflow conditions are given. Snapshots of vorticity and pressure are also presented. The flowfields are shown in Sec. III, with two subsections devoted to the shear-layer zone and to the jet development. The acoustic fields are reported in Sec. IV, and possible links with the flow properties are suggested. Finally, conclusions are drawn in Sec. V.

## II. Simulation Parameters

### A. Numerical Procedure

The numerical algorithm is identical to that of the earlier simulation[18,19] of the $M = 0.9$, $Re_D = 4 \times 10^5$ jet. The filtered compressible Navier–Stokes equations are solved using highly accurate numerical schemes with low dispersion and low dissipation properties.[21] A 13-point finite difference scheme is used for spatial discretization, whereas an explicit six-stage Runge–Kutta algorithm is applied for time integration. Grid-to-grid oscillations are removed by an explicit filtering that is optimized to damp only the short waves discretized by less than four points per wavelength. This filtering is used to ensure numerical stability and also to take into account the effects of the subgrid energy-dissipating scales without affecting the resolved scales. This approach was developed to preserve the Reynolds number of the jet, which might not be possible using eddy-viscosity models. It was indeed shown in a previous work[20] that the effective flow Reynolds number is artificially decreased using the dynamic Smagorinsky model, whereas it corresponds well to the initial jet conditions using the filtering alone. Furthermore, to compute the noise directly, nonreflective boundary conditions are implemented, with the addition of a sponge zone[22] at the outflow.

The numerical parameters of the present simulations are those of the simulation referred to as LESac in recent papers.[18,19] The computational domain is discretized by a 12.5 million point Cartesian grid with 15 points in the jet radius $r_0$. The flow is computed up to an axial distance of $25r_0$. The sound field is calculated radially up to $15r_0$ from the jet axis, and resolved for Strouhal numbers $Sr = f D/u_j < 2$. Finally, the simulation time $T$ is long enough to achieve convergence of results, as shown, for instance, by the corresponding Strouhal number $D/(T u_j) = 9.9 \times 10^{-4}$.

### B. Definition of Inflow Conditions

Initial conditions are defined for an isothermal round jet with a centerline velocity $u_j$ and a diameter $D = 2r_0$, yielding a Mach number $M = u_j/c_a = 0.9$ and a Reynolds number $Re_D = u_j D/\nu = 4 \times 10^5$. The mean profiles of velocities, pressure, and density are imposed at the inflow boundary. The axial velocity is given by a hyperbolic-tangent profile describing an annular shear layer of radius $r_0$ and of momentum thickness $\delta_\theta$. Radial and azimuthal velocities are set to zero, pressure is set to the ambient pressure, and the mean density profile is obtained from a Crocco–Buseman relation. All mean inflow profiles are imposed at the Cartesian grid nodes as described in previous work.[18,19] They are expected to be well resolved given the accuracy of the numerical schemes used.

To start the turbulence transition, disturbances are added to the velocity profiles in the shear-layer zone. They are divergence free and have a low amplitude to minimize spurious acoustic waves. The inflow forcing is based on a combination of the jet azimuthal modes, and it modifies the axial and radial velocities every time step in the following way:

$$\begin{Bmatrix} u \\ v \end{Bmatrix} = \begin{Bmatrix} u \\ v \end{Bmatrix} + \alpha u_j \sum_{i=n}^{m} \epsilon_i \cos(i\phi + \phi_i) \begin{Bmatrix} u^{\text{ring}} \\ v^{\text{ring}} \end{Bmatrix}$$

where the amplitudes $-1 \le \epsilon_i \le 1$ and the phases $0 \le \phi_i \le 2\pi$ of each mode are randomly updated every iteration. The unit vortex ring velocities are expressed, for $r = \sqrt{(y^2 + z^2)} \neq 0$, as

$$\begin{Bmatrix} u^{\text{ring}} \\ v^{\text{ring}} \end{Bmatrix} = \frac{2r_0}{r\Delta y} \exp\left[-\ell n(2)\frac{\Delta(x, r)^2}{\Delta y^2}\right] \begin{Bmatrix} r - r_0 \\ x_0 - x \end{Bmatrix}$$

where $\Delta(x, r)^2 = (x - x_0)^2 + (r - r_0)^2$, $\Delta y$ is the transverse grid spacing, and the axial location is $x_0 \simeq r_0$. Note that a large part of the forcing disturbances is damped because of the random updating. This forcing procedure was first used for a moderate Reynolds number jet[14] with $\alpha = 0.01$, $n = 0$, and $m = 9$.

In the present study, four simulations are carried out with the inflow conditions listed in Table 1. The parameters ($\delta_\theta = 0.05r_0$, $\alpha = 0.007$, $n = 0$, and $m = 15$) of the simulation[18,19] referred to as LESac are changed in three new simulations: The amplitude $\alpha$ is halved in the LESampl simulation, the shear layer is significantly thinner in the LESshear simulation with $\delta_\theta = 0.03r_0$, and the first four modes from $i = 0$ to 3 are removed in the forcing of the LESmode simulation.

### C. Instantaneous Vorticity and Pressure

Figures 1 and 2 present snapshots of the vorticity norm and of the fluctuating pressure for the four simulations. The flow developments from transitional shear layers to turbulent jets appear to be fairly similar, but also more or less rapid according to the inflow conditions. The jet seems to develop faster in the LESshear simulation and slower in the LESmode simulation. These observations are supported by the mean centerline axial velocities $u_c$, to be shown later, and by the potential core lengths $x_c$ defined here by $u_c(x_c) = 0.95u_j$, which are given in Table 2 but which will be discussed further.

**Table 1 Inflow conditions of the different simulations**

| Reference | $\delta_\theta/r_0$ | $\alpha$ | Modes |
|---|---|---|---|
| LESac | 0.05 | 0.007 | $i = 0, \ldots, 15$ |
| LESampl | 0.05 | 0.0035 | $i = 0, \ldots, 15$ |
| LESshear | 0.03 | 0.007 | $i = 0, \ldots, 15$ |
| LESmode | 0.05 | 0.007 | $i = 4, \ldots, 15$ |

**Table 2 Potential core lengths obtained for the different simulations**

| Reference | $x_c$ |
|---|---|
| LESac | $10.2r_0$ |
| LESampl | $10.6r_0$ |
| LESshear | $9.8r_0$ |
| LESmode | $11.9r_0$ |

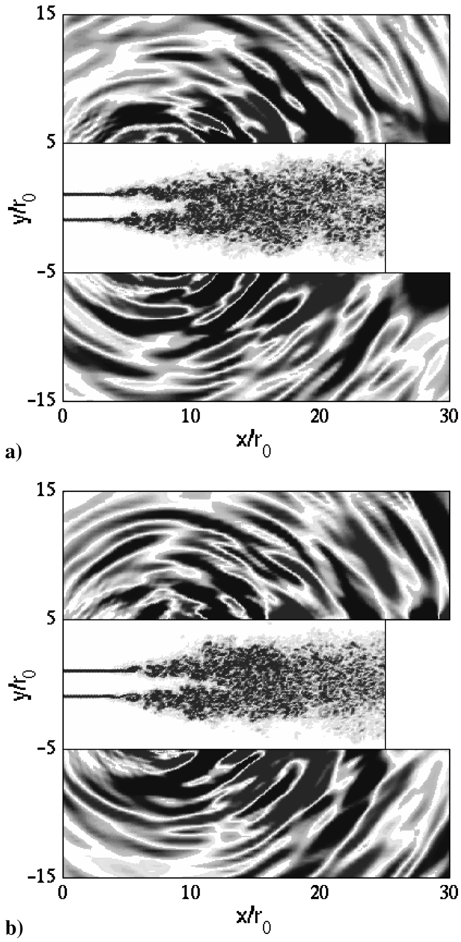


**Fig. 1 Snapshots of vorticity $|\omega|$ in the flow and of fluctuating pressure $p'$ outside, in $x$–$y$ plane at $z = 0$ for simulations: a) LESac and b) LESampl; color scales are from 0 to $8 \times 10^4$ s$^{-1}$ for vorticity and from $-70$ to 70 Pa for pressure.**

Changes in the radiated sound fields are also visible in the pressure snapshots.Whereas the sound radiations for the LESac and for the LESampl simulations seem not to differ significantly, the radiations for the LESshear and for the LESmode simulations appear to be, respectively, enhanced and reduced, particularly in the sideline and upstream directions.

## III. Flow Properties

### A. Shear Layer Development

The streamwise variations of the shear-layer vorticity thickness $\delta_\omega$ are shown in Fig. 3 for the different simulations. This characteristic thickness is calculated from the mean axial velocity $\langle u\rangle$ using $\delta_\omega = u_j/\max(|\partial\langle u\rangle/\partial y|)$, and it is related to the momentum thickness for a hyperbolic-tangent profile by $\delta_\omega = 4\delta_\theta$. For the three simulations LESac, LESshear, and LESampl, the shear layer spreads earlier with the smaller initial thickness as observed experimentally by Hussain and Zedan[5] and later with the decreased forcing amplitude. Similar growth rates, $d\delta_\omega/dx$, are found, with a value of about 0.22 in the range of the higher rates provided in the literature.[4] Therefore, the discrepancies in their respective core lengths reported in Table 2 can be attributed mainly to the shifted locations of the

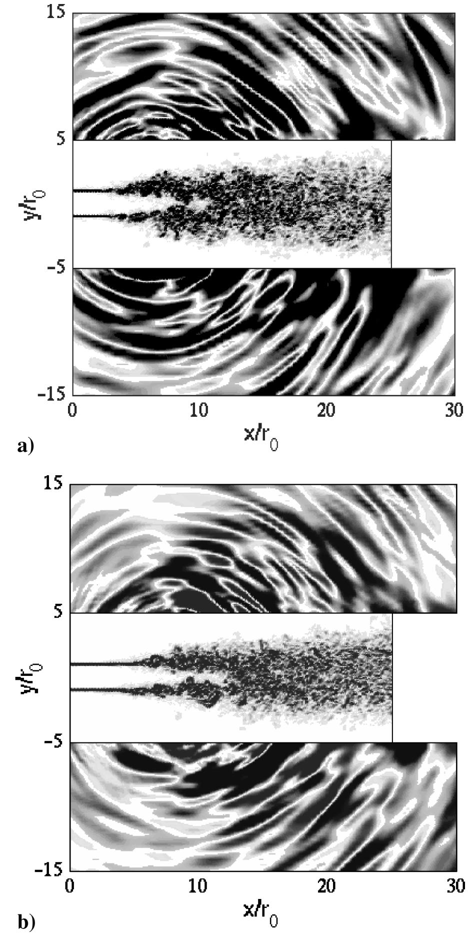


**Fig. 2 Snapshots of vorticity and of fluctuating pressure for simulations: a) LESshear and b) LESmode; see Fig. 1 caption for details.**

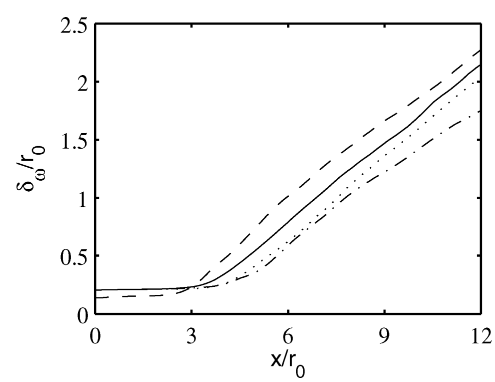


**Fig. 3 Axial evolution of vorticity thickness $\delta_\omega$: ——, LESac; · · · ·, LESampl; – – –, LESshear; and — · —·, LESmode.**

spreading starting points. For the LESmode simulation, the shear layer appears to develop even later and more slowly. Two regions of spreading are visible: The vorticity thickness grows rapidly up to $x \simeq 8r_0$, then the rate of growth progressively decreases to reach $d\delta_\omega/dx \simeq 0.18$ for $10r_0 \leq x \leq 12r_0$. This behavior and this rate are in good agreement with the measurements by Husain and Hussain[6] for transitional axisymmetric shear layers.

The $u'$ velocity spectra for $x = 3r_0$ and $r = r_0$ are presented in Fig. 4 to investigate the preliminary stage of the shear-layer development. They are marked by the instability waves growing in the inflow velocity profiles. The peak for LESshear is found at a Strouhal number of $Sr \simeq 0.9$ and those for LESac and LESampl at $Sr \simeq 0.6$. These values compare favorably with the Strouhal numbers, $Sr = 1.13$ and 0.68, associated with the most unstable axisymmetric modes of the inflow shear layers predicted by the linear instability theory.[23] The discrepancies could be due to nonlinear

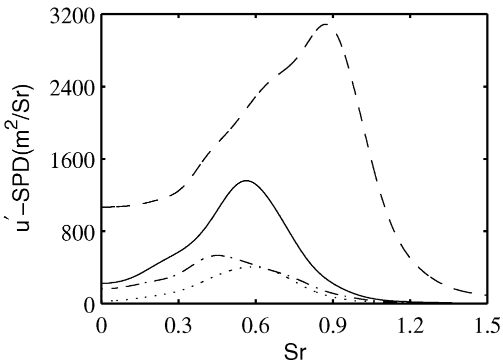


**Fig. 4 Spectral power densities of $u'$ velocity as a function of Strouhal number $Sr = fD/u_j$, for $x = 3r_0$ and $r = r_0$, in linear scales: ——, LESac; · · · ·, LESampl; – – –, LESshear; and –· –·, LESmode.**

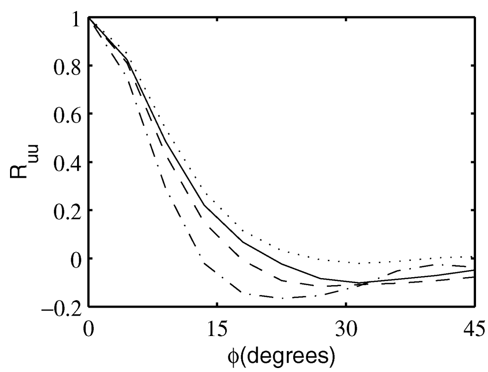


**Fig. 5 Azimuthal cross-correlation functions of the fluctuating axial velocity for $x = 6r_0$ and $r = r_0$: ——, LESac; · · · ·, LESampl; – – –, LESshear; and –·–·, LESmode.**

effects and to the differences between the velocity profiles at the inflow and at $x = 3r_0$. The peak amplitude is higher for the thinner initial shear layer, which illustrates that the instability amplification is stronger as $\delta_\theta$ decreases.[23] By the use of a smaller forcing magnitude in LESampl, the peak amplitude with respect to LESac is reduced, without affecting its frequency, suggesting that the same development occurs. For LESmode, a less pronounced peak is observed for a lower Strouhal number of $Sr \simeq 0.45$. This indicates that the initial shear-layer development may not be governed by the same instability modes in the two cases.

To study the azimuthal turbulence structures, the cross-correlation functions $R_{uu}(\phi)$ of the $u'$ velocity are calculated in the shear layer for $r = r_0$ at an axial distance $x = 6r_0$. They are presented in Fig. 5 for an azimuth $0 \leq \phi \leq 45$ deg. For the three simulations using the same modal excitation, the correlation is higher for LESampl and lower for LESshear, where the shear-layer transitions occur later and earlier, respectively. These observations suggest that the azimuthal correlation decreases as the turbulence transition continues. The results obtained for LESmode seem to disagree with this trend because the correlation is much lower than that for the three previous simulations, with yet a later shear-layer development. However, the results clearly show that the turbulence generated using the forcing involving only the higher modes $i \geq 4$ has a more three-dimensional structure than that using the forcing with all of the modes $i \geq 0$.

The streamwise profiles for $r = r_0$ of the rms fluctuating axial and radial velocities are presented in Fig. 6. The axial locations and the magnitudes of their peaks are investigated. For each of the three simulations LESshear, LESac, and LESampl, the $u'_{\mathrm{rms}}$ and the $v'_{\mathrm{rms}}$ peaks occur at similar streamwise distances, respectively, at $x \simeq 4.5r_0$, $x \simeq 6r_0$, and $x \simeq 7r_0$, according to the shifts in shear-layer development observed earlier. For the LESmode simulation, however, the two peaks do not coincide: Here, $u'_{\mathrm{rms}}$ reaches its maximum value at $x \simeq 6r_0$ whereas $v'_{\mathrm{rms}}$ does so farther downstream at $x \simeq 7r_0$.

**Table 3 RMS peak values of the fluctuating velocity profiles for $r = r_0$**

| Reference | $(u'_{\mathrm{rms}})_p{}^{a}/u_j$ | $(v'_{\mathrm{rms}})_p/u_j$ | $(v'_{\mathrm{rms}})_p/(u'_{\mathrm{rms}})_p$ |
|---|---|---|---|
| LESac | 0.203 | 0.186 | 0.92 |
| LESampl | 0.209 | 0.190 | 0.91 |
| LESshear | 0.212 | 0.196 | 0.92 |
| LESmode | 0.200 | 0.168 | 0.84 |

[a]Subscript $p$ used for peak.

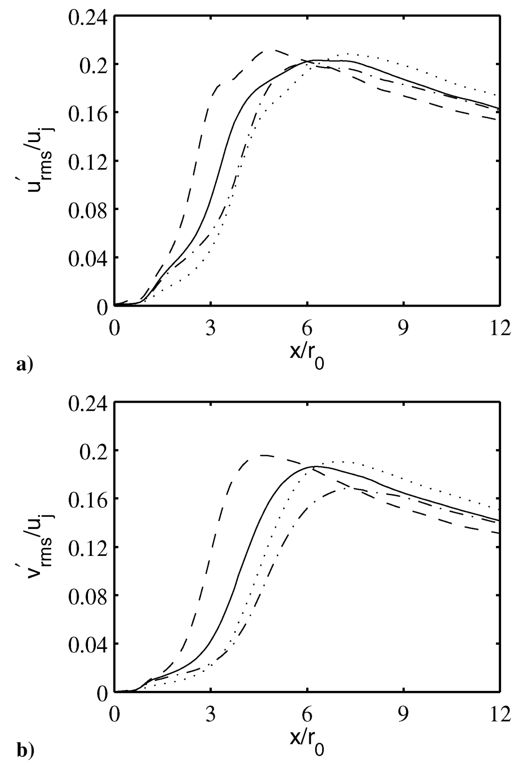


**Fig. 6 Axial profiles for $r = r_0$ of rms values of fluctuating velocities a) $u'$ and b) $v'$: ——, LESac; · · · ·, LESampl; – – –, LESshear; and –·–·, LESmode.**

The magnitudes of the peaks are listed in Table 3. Similar peak values are found for the axial velocity, in fairly good agreement with measurements by Hussain and Zedan[5] reporting $(u'_{\mathrm{rms}})_p/u_j \simeq 0.19$ in transitional axisymmetric shear layers. The peak values obtained for the radial velocity are more scattered and are all higher than the $(v'_{\mathrm{rms}})_p/u_j \simeq 0.13$ measured by Hussain and Husain[7]. The ratios between the $v'_{\mathrm{rms}}$ and $u'_{\mathrm{rms}}$ peak magnitudes are also provided in Table 3. A ratio of about 0.92 is noted for the simulations LESac, LESampl, and LESshear, whereas a smaller ratio is found for LESmode.

These results indicate that the turbulent shear layers have an identical structure for the three simulations using the same modal forcing. The magnitudes of velocity fluctuations are only slightly enhanced when the initial shear-layer thickness is smaller or when the forcing amplitude is decreased. For the LESmode simulation, the turbulent shear layer displays quite different properties, with a significant reduction of the magnitude of the radial fluctuating velocity.

### B. Jet Development

The influence of the inflow conditions on the jet development just after the potential core is now investigated. The streamwise evolutions of the mean centerline velocity $u_c$ and of the jet half-width $\delta_{0.5}$ are presented in Fig. 7 for the different simulations. The potential core lengths $x_c$, arbitrarily defined by $u_c(x_c) = 0.95u_j$, are about $10r_0$ for LESac, LESampl, and LESshear, but are $12r_0$ for LESmode (Table 2). The core lengths compare favorably with those observed for untripped jets at similar Reynolds numbers by Raman et al.[8] and Arakeri et al.,[12] that is, $x_c \simeq 10r_0$ and $x_c \simeq 14r_0$,

**Table 4 RMS peak values of centerline fluctuating velocity profiles**

| Reference | $(u'_{\mathrm{rms}})_{p^a}/u_j$ | $(v'_{\mathrm{rms}})_p/u_j$ | $(v'_{\mathrm{rms}})_p/(u'_{\mathrm{rms}})_p$ |
|---|---|---|---|
| LESac | 0.131 | 0.118 | 0.90 |
| LESampl | 0.137 | 0.124 | 0.91 |
| LESshear | 0.122 | 0.113 | 0.91 |
| LESmode | 0.120 | 0.106 | 0.88 |

[a]Subscript $p$ used for peak.

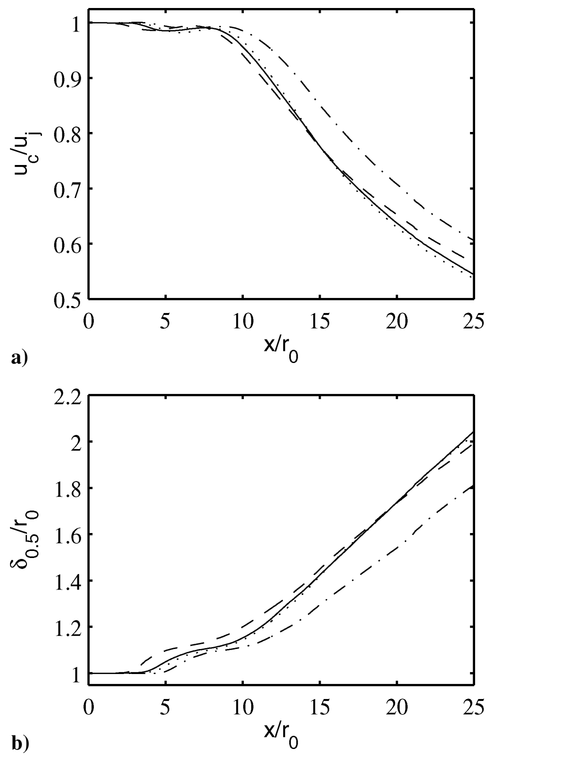


**Fig. 7 Axial profiles a) of mean centerline velocity $u_c/u_j$ and b) of jet half-width $\delta_{0.5}/r_0$: ——, LESac; · · · ·, LESampl; – – –, LESshear; and –·–·, LESmode.**

respectively. They are all smaller than those found for higher Reynolds number, turbulent jets[24,25] yielding $x_c \simeq 14r_0$. This result is in agreement with experiments by Raman et al.,[8] showing that the potential core is shorter in an initially transitional jet than in an initially turbulent jet.

The effects of the shear-layer thickness and of the forcing amplitude on the centerline velocity decay and on the jet spreading are similar to the direct numerical simulation (DNS) results documented by Stanley and Sarkar[13] for a low Reynolds number plane jet. The jets for LESac and for LESampl using a smaller forcing amplitude develop at nearly the same rate. The decrease in the shear-layer thickness for LESshear has a more significant impact on the jet development, which clearly occurs at a lower rate than in LESac. For the LESmode using the higher-mode excitation, the jet develops even more slowly. When experimental observations[8] that the spreading rate is higher in an initially transitional jet than in an initially turbulent jet are taken into account, this may suggest that the jet excited with higher modes behaves more like a turbulent jet than the other three jets. Note that no decay or spreading rate is provided here because these rates are significant only in the self-similarity region that is reached farther downstream.[18,19,26]

The rms values of the axial and radial fluctuating velocities on the jet axis are shown in Fig. 8. For each of the four simulations, the peaks for $u'_{\mathrm{rms}}$ and for $v'_{\mathrm{rms}}$ are found at the same streamwise distance, at around five radii downstream from the end of the potential core, as observed experimentally in Ref. 12, for instance. The peak values are listed in Table 4. They agree well with the experimental data, both for the axial and the radial velocities. For $u'_{\mathrm{rms}}/u_j$, maxima of 0.13 and 0.12 were measured for similar Reynolds number, untripped

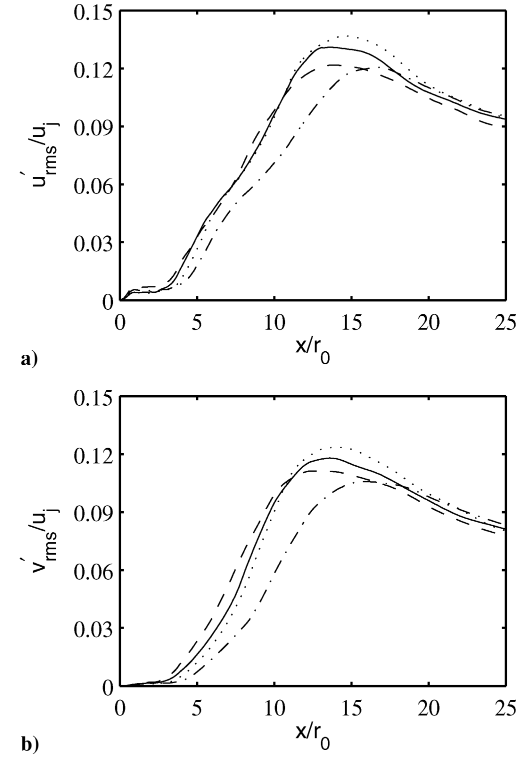


**Fig. 8 Centerline profiles of rms value of fluctuating velocities a) $u'$ and b) $v'$: ——, LESac; · · · ·, LESampl; – – –, LESshear; and –·–·, LESmode.**

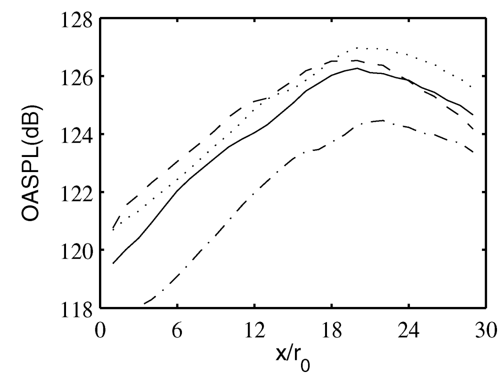


**Fig. 9 Overall sound pressure levels for $r = 15\ r_0$: ——, LESac; · · · ·, LESampl; – – –, LESshear; and –·–·, LESmode.**

jets[8,12] and maxima of 0.14 and 0.13 were measured for $Re_D = 10^6$ turbulent jets.[24,25] For $v'_{\mathrm{rms}}/u_j$, peak values of 0.11 and 0.1 were reported in the latter cases.

The effects of the inflow conditions on the centerline turbulence peak values are clearly visible. The use in LESampl of a forcing amplitude smaller than in LESac enhances the turbulence peaks, whereas that of a thinner initial shear layer in LESshear leads to a reduction, in accordance with the trends found in the DNS by Stanley and Sarkar.[13] The forcing using higher modes in LESmode decreases the peak values both for $u'_{\mathrm{rms}}$ and for $v'_{\mathrm{rms}}$. The ratios between the $v'_{\mathrm{rms}}$ and the $u'_{\mathrm{rms}}$ maxima are provided in Table 4. They are found to be 0.88 in LESmode and about 0.92 in the other simulations, which shows that the turbulence structure just after the potential core differs according to the modes involved in the inflow disturbances. The influence of the forcing modal properties on turbulence anisotropy appears, however, to be weaker than it is earlier in the shear-layer zones.

## IV. Acoustic Fields

### A. Overall Sound Pressure Levels

The profiles for $r = 15r_0$ of the sound pressure levels given directly by the LES are presented in Fig. 9. The effects of the inflow conditions on the amplitude of the radiated noise are clearly shown. The decrease of the forcing magnitude in LESampl results in an amplification of the sound field by about 1 dB with respect to LESac. This amplification appears to be almost uniform for $0 \leq x \leq 30r_0$. The modification of the sound field when using a thinner shear-layer momentum thickness is different. The sound levels in LESshear are increased with respect to LESac for $x \leq 24r_0$, but they are reduced farther downstream for $x \geq 24r_0$. This change according to the direction of sound emission lead us to investigate in subsequent subsections the properties of the sound field in the downstream and sideline directions where two distinct noise components are likely to be dominant.[27] A significant noise reduction of about 2 dB is obtained in the LESmode simulation using a higher mode excitation. This result corresponds well to the behavior found by Bodony and Lele,[15] who reported that forcing using only the first three azimuthal modes is not sufficient and yields overestimated noise levels. At this point, note that the sound levels are shown to depend appreciably on the different inflow parameters. Because they also appear to be dependent on the subgrid modelings,[20] great care is to be taken when the sound pressure levels are used to demonstrate the validity of a jet noise prediction by LES.

### B. Downstream Noise Properties

Spectra and azimuthal correlation functions of the acoustic fields are calculated for $x = 29r_0$ and $r = 12r_0$, as in earlier papers.[18,19] They are presented in Fig. 10. The shapes of the spectra are quite similar, with peaks observed for Strouhal numbers $Sr \simeq 0.3$ in agreement with experimental data.[25,28] The very close peak frequencies in the four simulations suggest that the source mechanism of the downstream noise is the same for all of the inflow conditions. This is also supported by the cross-correlation functions of the fluctuating pressure $R_{pp}(\phi)$, which display no significant differences according to the initial conditions. These correlation functions are typical[18,19] of measurements[29] at angles of $\theta \simeq 30$ deg from the jet axis. Also note that the more correlated the sound field, the higher the peak amplitude of the sound spectra.

The sound levels calculated from the spectra at $x = 29r_0$ and $r = 12r_0$ are listed in Table 5. The levels are higher for LESampl

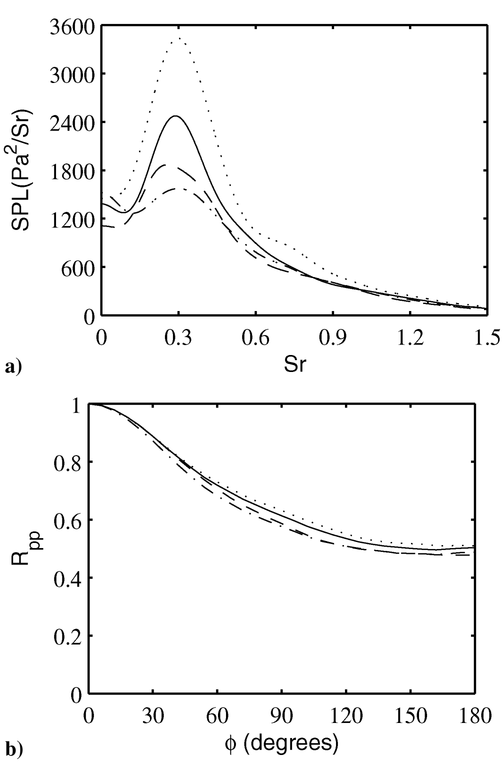


**Fig. 10 For $x = 29r_0$ and $r = 12\ r_0$, a) sound pressure spectra in linear scales as function of Strouhal number $Sr = fD/u_j$ and b) azimuthal cross correlations of fluctuating pressure: ——, LESac; · · · ·, LESampl; – – –, LESshear; and –·–·, LESmode.**

**Table 5 Sound pressure levels in decibels[a]**

| Reference | $x = 29r_0$ $r = 12r_0$ | $d = 60r_0$ $\theta \simeq 30$ deg |
|---|---|---|
| LESac | 125.2 | 116.7 |
| LESampl | 126.5 | 118 |
| LESshear | 124.5 | 116 |
| LESmode | 124.5 | 116 |

[a]Left: $x = 29r_0$ and $r = 12r_0$, and right: $\theta \simeq 30$ deg at a distance $d = 60r_0$ from an origin taken as $x = 10r_0$ and $r = 0$, using $1/d$ decay law.

and lower for LESshear and LESmode, as was already observed on the sound spectra. For a simple comparison with experiments, the sound levels are extrapolated at a distance of $d = 60r_0$ from a source region assumed to be at $x = 10r_0$ on the jet axis, at the end of the potential core.[14] The radiation angle thus defined from the jet axis is $\theta \simeq 30$ deg. The levels are calculated using the $1/d$ decay law of sound waves and are given in Table 5. They agree with the measurements for Mach 0.9, high Reynolds number jets at $\theta \simeq 30$ deg (115.5 dB, Jordan et al.[25]; 116.3 dB, Mollo-Christensen et al.[28]; and 114.6 dB, Tanna[30]) even if the 118-dB level predicted by the LESampl simulation seems slightly overestimated.

We now try to connect the noise to the flow disturbance magnitude. This idea was developed in particular by Zaman,[31] who showed that the noise sources in an $M = 0.5$, $Re_D = 3 \times 10^5$ jet could be represented by the turbulence maxima locations. Arakeri et al.,[12] using microjets for an $M = 0.9$ jet, also observed that the reduction of the sound levels accompanies the decrease of the turbulence intensities. Because the sources responsible for the downstream noise are expected to be located just after the end of the potential core,[14] we focus our attention on the peaks of centerline turbulence intensities that occur about two diameters after the jet core. The variations of the centerline turbulence maxima, shown earlier in Fig. 8 and listed in Table 4, are found to follow exactly those of the peak values for $Sr \simeq 0.3$ in the sound spectra. This observation supports that the downstream noise component is associated with the turbulence intruding into the jet past the end of the potential core.[14] The downstream sound levels are then just a function of the centerline turbulence intensity maxima.

### C. Sideline Noise Properties

The properties of the sound fields in the sideline direction are now investigated. For high Reynolds number jets, they differ significantly from those in the downstream direction, in terms of spectral contents[32] and azimuthal correlations.[29] This important behavior was shown to be obtained in the present LES.[18,19]

Sound spectra and cross-correlation functions are calculated for $x = 11r_0$ and $r = 15r_0$ and are presented in Fig. 11. The four spectra display similar broadband shapes with peaks for Strouhal numbers $Sr \simeq 0.6$–$0.7$. The azimuthal correlation functions shown for $0 \leq \phi \leq 60$ deg are also very close, which supports that the same sound-generation mechanisms take place in the four simulations. The decrease of the shear-layer thickness in LESshear enhances the sideline high-frequency noise, which is to be expected because this noise component is mainly generated in the shear layers just after the nozzle exit.[31] The use of a smaller forcing amplitude in LESampl slightly also increases the acoustic levels. However, the most striking change with respect to LESac is obtained from the LESmode simulation with a significant noise reduction.

The levels calculated from the previous spectra are given in Table 6. They are roughly extrapolated in the far field, using the $1/d$ decay law of acoustic waves from an arbitrary source region. After a careful examination of the snapshots of pressure fields in Figs. 1 and 2, the origin is chosen to be at $x = 7r_0$ on the jet axis. It defines an angle of sound emission from the jet axis of $\theta \simeq 75$ deg. The sound levels extrapolated at a distance $d = 60r_0$ are provided in Table 6. They are found to be about 4 dB higher than the corresponding measurements at $\theta \simeq 75$ deg (106 dB, Jordan et al.[25]; 108.2 dB, Mollo-Christensen et al.[28]; and 108.3 dB, Tanna[30]), the 110-dB level provided by the LESmode simulation being the closest.

**Table 6 Sound pressure levels in decibels[a]**

| Reference | $x = 11r_0$, $r = 15r_0$ | $d = 60r_0$, $\theta \simeq 75$ deg |
|---|---|---|
| LESac | 124.1 | 112.3 |
| LESampl | 124.7 | 113 |
| LESshear | 125.2 | 113.4 |
| LESmode | 121.8 | 110 |

[a]Left: $x = 11r_0$ and $r = 15r_0$, and right: $\theta \simeq 75$ deg at a distance $d = 60r_0$ from an origin taken as $x = 7r_0$ and $r = 0$, using $1/d$ decay law.

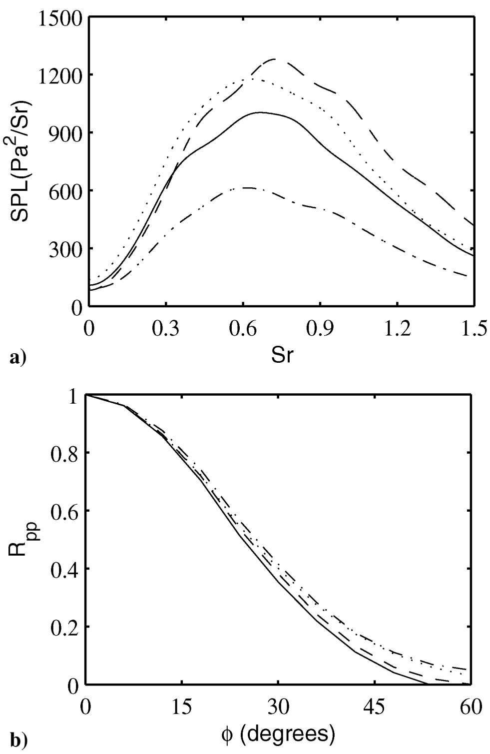


**Fig. 11 For $x = 11\ r_0$ and $r = 15\ r_0$, a) sound pressure spectra in linear scales as function of Strouhal number $Sr = fD/u_j$ and b) azimuthal cross correlations of fluctuating pressure: ——, LESac; · · · ·, LESampl; – – –, LESshear; and –·–·, LESmode.**

Because the shear-layer turbulence is expected to contribute appreciably to the sideline noise, it seems natural to relate the present overestimated sound levels to the excessive magnitudes of the radial velocity fluctuations in the shear layer. It is found that the sound levels of Table 6 vary accurately as the maxima of $v'_{\mathrm{rms}}$ presented in Fig. 6 and listed in Table 3. The sideline noise is shown to be linked to the intensity of the radial velocity disturbances in the shear layer. For proper prediction of sideline noise levels in numerical simulations, it appears necessary to continue to define an inflow forcing that reduces this quantity. The results from the LESmode simulation suggest, however, that the first jet modes should not be involved when synthesizing the initial perturbations.

## V. Conclusions

This paper describes effects of the inflow conditions for a high subsonic, $Re_D = 4 \times 10^5$ circular jet simulated by LES. Both the flow development and the emitted sound are shown to depend appreciably on the initial parameters chosen to model the inflow of this transitional jet.

The reduction of the amplitude of the initial disturbances is found to alter the flow and sound properties only weakly and in the following way: The jet development occurs slightly downstream with higher turbulence intensities and, consequently, results in an increased radiated noise. The use of a thinner shear-layer momentum thickness leads to more significant and complex modifications. The transition is more rapid and turbulence intensities are increased in the shear layer, but the jet development is slower and the intensities are decreased after the potential core. As a result, noise is enhanced in the sideline direction but reduced in the downstream direction. The most important changes in the flow features are obtained with the removal of the first four jet azimuthal modes in the construction of the inflow disturbances: The jet develops much later and more slowly, and turbulence intensities and noise levels are notably reduced. This work demonstrates the importance of the modeling of the inflow conditions for high Reynolds number jets. In particular, initial conditions are still to be tested that reduce the sideline pressure levels that are currently overestimated with respect to experimental data. This discrepancy has been connected to the high intensity of the radial fluctuating velocity in the shear layer.

Strong links between the turbulence and the sound radiation are indeed suggested by the present simulations. The levels of the downstream noise dominated by an $Sr \simeq 0.3$ peak can be related to the maxima of centerline intensities just after the potential core, which suggests that the associated noise source is effectively located in this zone. The amplitudes of the sideline noise are also found to be connected to the peak values of the radial velocity fluctuations in the shear layer. The broadband noise generated in the sideline direction for jets at high Reynolds numbers is, thus, shown to be direcly associated to the development of the shear-layer turbulence.

## Acknowledgments

This work was supported by the European Union Research program Jet Exhaust Aerodynamics and Noise, Contract G4RD-CT-2000-00313, and by the French program Recherche Aéronautique sur le Supersonique, Ministère de la Recherche. Computing time was supplied by the Institut du Développement et des Ressources en Informatique Scientifique, Centre National de la Recherche Scientifique.

## References

[1]Crighton, D. G., "Acoustics as a Branch of Fluid Mechanics," *Journal of Fluid Mechanics*, Vol. 106, 1981, pp. 261–298.

[2]Zaman, K. B. M. Q., "Far-field Noise of a Subsonic Jet Under Controlled Excitation," *Journal of Fluid Mechanics*, Vol. 152, 1985, pp. 83–111.

[3]Hill, W. G., Jr., Jenkins, R. C., and Gilbert, B. L., "Effects of the Initial Boundary-Layer State on Turbulent Mixing," *AIAA Journal*, Vol. 14, No. 11, 1976, pp. 1513, 1514.

[4]Gutmark, E., and Ho, C.-M., "Preferred Modes and the Spreading Rates of Jet," *Physics of Fluids*, Vol. 26, No. 10, 1983, pp. 2932–2938.

[5]Hussain, A. K. M. F., and Zedan, M. F., "Effects of the Initial Condition on the Axisymmetric Free Shear Layer: Effects of the Initial Momentum Thickness," *Physics of Fluids*, Vol. 21, No. 7, 1978, pp. 1100–1112.

[6]Husain, Z. D., and Hussain, A. K. M. F., "Axisymmetric Mixing Layer: Influence of the Initial and Boundary Conditions," *AIAA Journal*, Vol. 17, No. 1, 1979, pp. 48–55.

[7]Hussain, A. K. M. F., and Husain, Z. D., "Turbulence Structure in the Axisymmetric Free Mixing Layer," *AIAA Journal*, Vol. 18, No. 12, 1980, pp. 1462–1469.

[8]Raman, G., Rice, E. J., and Reshotko, E., "Mode Spectra of Natural Disturbances in a Circular Jet and the Effect of Acoustic Forcing," *Experiments in Fluids*, Vol. 17, No. 6, 1994, pp. 415–426.

[9]Xu, G., and Antonia, R. A., "Effects of Different Initial Conditions on a Turbulent Free Jet," *Experiments in Fluids*, Vol. 33, No. 5, 2002, pp. 677–683.

[10]Bridges, J. E., and Hussain, A. K. M. F., "Roles of Initial Conditions and Vortex Pairing in Jet Noise," *Journal of Sound and Vibration*, Vol. 117, No. 2, 1987, pp. 289–311.

[11]Simonich, J. C., Narayanan, S., Barber, T. J., and Nishimura, M., "Aeroacoustic Characterization, Noise Reduction, and Dimensional Scaling Effects of High Subsonic Jets," *AIAA Journal*, Vol. 39, No. 11, 2001, pp. 2062–2069.

[12]Arakeri, V. H., Krothapalli, A., Siddavaram, V., Alkislar, M. B., and Lourenco, L., "On the Use of Microjets to Suppress Turbulence in a Mach 0.9 Axisymmetric Jet," *Journal of Fluid Mechanics*, Vol. 490, 2003, pp. 75–98.

[13]Stanley, S. A., and Sarkar, S., "Influence of Nozzle Conditions and Discrete Forcing on Turbulent Planar Jets," *AIAA Journal*, Vol. 38, No. 9, 2000, pp. 1615–1623.

[14]Bogey, C., Bailly, C., and Juvé, D., "Noise Investigation of a High Subsonic, Moderate Reynolds Number Jet Using a Compressible LES," *Theoretical and Computational Fluid Dynamics*, Vol. 16, No. 4, 2003, pp. 273–297.

[15]Bodony, D. J., and Lele, S. K., "Influence of Inlet Conditions on the Radiated Noise of High Speed Turbulent Jets," Workshop LES for Acoustics, DLR, Göttingen, Germany, Oct. 2002; also AIAA Paper 2001-0376, Jan. 2001.

[16]Chyczewski, T. S., Long, L. N., and Morris, P. J., "Numerical Study of Nozzle Exit Conditions Effects on Jet Development," *AIAA Journal*, Vol. 36, No. 6, 1998, pp. 986–993.

[17]Boersma, B. J., Brethouwer, G., and Nieuwstadt, F. T. M., "A Numerical Investigation on the Effect of the Inflow Conditions on a Self-Similar Region of a Round Jet," *Physics of Fluids*, Vol. 10, No. 4, 1998, pp. 899–909.

[18]Bogey, C., and Bailly, C., "Direct Computation of the Sound Radiated by a High Reynolds Number, Subsonic Round Jet," Confederation of European Aerospace Societies Workshop from CFD to CAA, Nov. 2002.

[19]Bogey, C., and Bailly, C., "Computation of a High Reynolds Number Jet and Its Radiated Noise Using LES Based on Explicit Filtering," *Computers and Fluids* (to be published).

[20]Bogey, C., and Bailly, C., "Decrease of the Effective Reynolds Number with Eddy-Viscosity Subgrid-Scale Modeling," *AIAA Journal*, Vol. 43, No. 2, 2005, pp. 437–439.

[21]Bogey, C., and Bailly, C., "A Family of Low Dispersive and Low Dissipative Explicit Schemes for Flow and Noise Computations," *Journal of Computational Physics*, Vol. 194, No. 1, 2004, pp. 194–214.

[22]Bogey, C., and Bailly, C., "Three-Dimensional Non Reflective Boundary Conditions for Acoustic Simulations: Far-Field Formulation and Validation Test Cases," *Acta Acustica*, Vol. 88, No. 4, 2002, pp. 463–471.

[23]Michalke, A., "Survey on Jet Instability Theory," *Progress in Aerospace Sciences*, Vol. 21, 1984, pp. 159–199.

[24]Lau, J. C., Morris, P. J., and Fisher, M. J., "Measurements in Subsonic and Supersonic Free Jets Using a Laser Velocimeter," *Journal of Fluid Mechanics*, Vol. 93, No. 1, 1979, pp. 1–27.

[25]Jordan, P., Gervais, Y., Valière, J.-C., and Foulon, H., "Final Results from Single Point Measurements," Project Deliverable D3.4, Jet Exhaust Aerodynamics and Noise–European Union 5th Framework Programme, Contract G4RD-CT2000-00313, April 2002.

[26]Wygnanski, I., and Fiedler, H., "Some Measurements in the Self-Preserving Jet," *Journal of Fluid Mechanics*, Vol. 38, No. 3, 1969, pp. 577–612.

[27]Tam, C. K. W., Golebiowski, M., and Seiner, J. M., "On the Two Components of Turbulent Mixing Noise from Supersonic Jets," AIAA Paper 96-1716, May 1996.

[28]Mollo-Christensen, E., Kolpin, M. A., and Martucelli, J. R., "Experiments on Jet Flows and Jet Noise Far-Field Spectra and Directivity Patterns," *Journal of Fluid Mechanics*, Vol. 18, 1964, pp. 285–301.

[29]Maestrello, L., "Two Points Correlations of Sound Pressure in the Far Field of a Jet: Experiment," NASA TMX-72835, April 1976.

[30]Tanna, H. K., "An Experimental Study of Jet Noise. Part I: Turbulent Mixing Noise," *Journal of Sound and Vibration*, Vol. 50, No. 3, 1977, pp. 405–428.

[31]Zaman, K. B. M. Q., "Flow Field and Near and Far Sound Field of a Subsonic Jet," *Journal of Sound and Vibration*, Vol. 106, No. 1, 1986, pp. 1–16.

[32]Lush, P. A., "Measurements of Subsonic Jet Noise and Comparison with Theory," *Journal of Fluid Mechanics*, Vol. 46, No. 3, 1971, pp. 477–500.

W. Ng
*Associate Editor*